9th Edition of the Large Hadron Collider Physics Conference
7th–12th June 2021

Jet Substructure + Correlations in Hadronic Final States from ATLAS

Robin Newhouse
University of British Columbia
On behalf of the ATLAS Collaboration

ATLAS EXPERIMENT

THE UNIVERSITY OF BRITISH COLUMBIA

2007.12600

Hadronic event shapes

Six event-shape variables are studied in multijet events . Multi-differential distributions are compared to MC simulation. Generators using ME beyond LO generators do well for high-p_T multijet events.

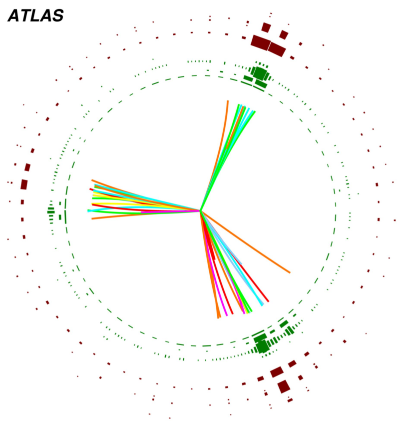

HEPData
Rivet

2004.03540

Lund jet plane

A double-differential cross-section measurement of the LJP is used to compare showering and hadronization algorithms. Physical effects can be factorized.

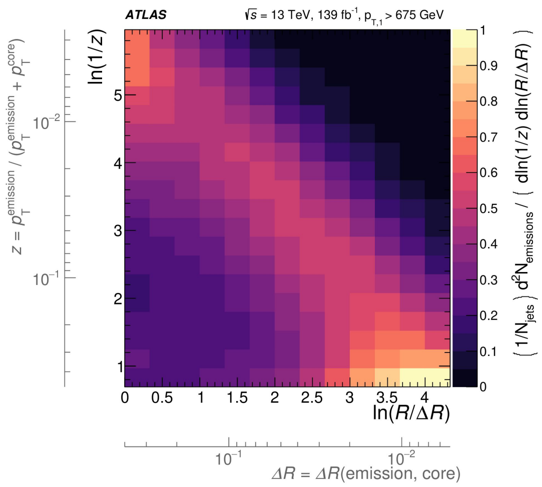

HEPData
Rivet

ATLAS-CONF-2020-025

α_s measurement using (A)TEEC

Transverse energy-energy correlations and their azimuthal asymmetries are studied in multi-jet events. QCD calculations are fitted to the distributions and the strong coupling constant is extracted for values up to 4 TeV.

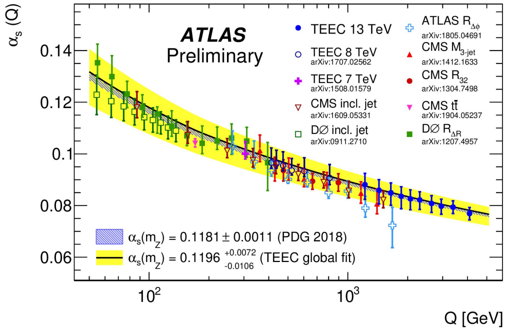

Coming soon

Hadronic event shapes

Event Shapes

Class of observables describing energy flow in multijet events

A good probe for strong-interaction processes

Great testing ground for multijet simulation

This measurement improves upon ATLAS Run-1 analysis (arXiv:1206.2135)

- 139 fb^{-1} of 13 TeV Run 2 data (>4000 x more!)
- High-p_T particle-flow jets
- Improved generators (ATL-PHYS-PUB-2019-017)

Analysis

- Single-jet trigger p_T > 460 GeV
- Particle-flow, anti-k_t jets, R = 0.4
  - p_T > 100 GeV
  - $|\eta| < 2.4$
- Events
  - ≥ 2 jets with H_{T2} > 1 TeV
  - $H_{T2} = p_{T1} + p_{T2}$
- Unfolding:
  - Unfolded to particle-level using iterative Bayesian unfolding

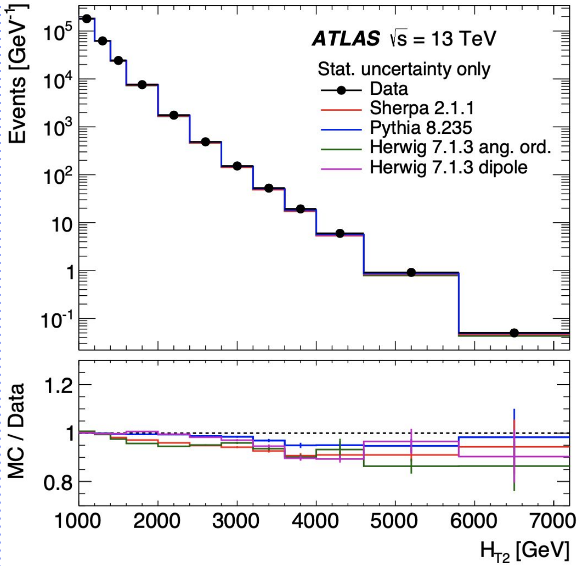

Scalar sum of transverse momenta of the two leading jets + MC predictions

2007.12600

Hadronic event shapes

Detailed definitions
in extra materials

Thrust

$T_{\perp}$: transverse

T_m: minor component

Measures back-to-back (dijet-like) configuration

Sphericity

S : spherical isotropic

$S_{\perp}$: transverse isotropic

Measures isotropic distribution of radiation

Aplanarity

A

Measures the containment of the radiation in a plane

C & D

C : quadratic combination

D : cubic combination

Quantities for 3+ and 4+ jet events

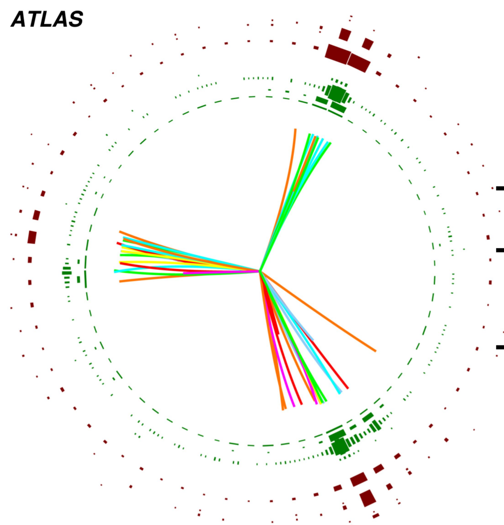

- 3-jet event
- High $\tau_{\perp}$ * (orthogonal energy flow)
- High $S_{\perp}$ (more spherical)

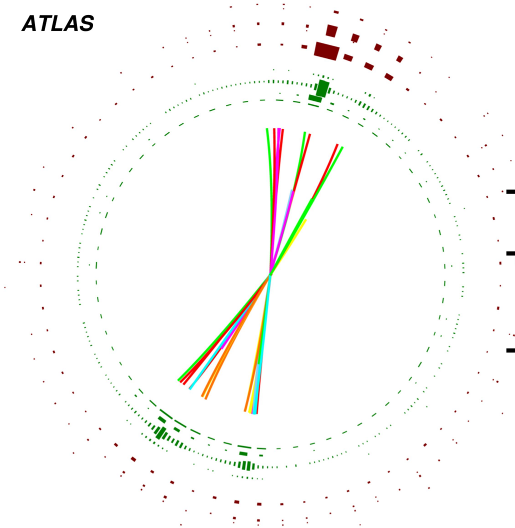

- 5-jet event
- Low $\tau_{\perp}$ * (dijet-like)
- Low $S_{\perp}$ (less spherical)

* $\tau_{\perp} = 1 - T_{\perp}$

Hadronic event shapes

$S_\perp$: Transverse sphericity

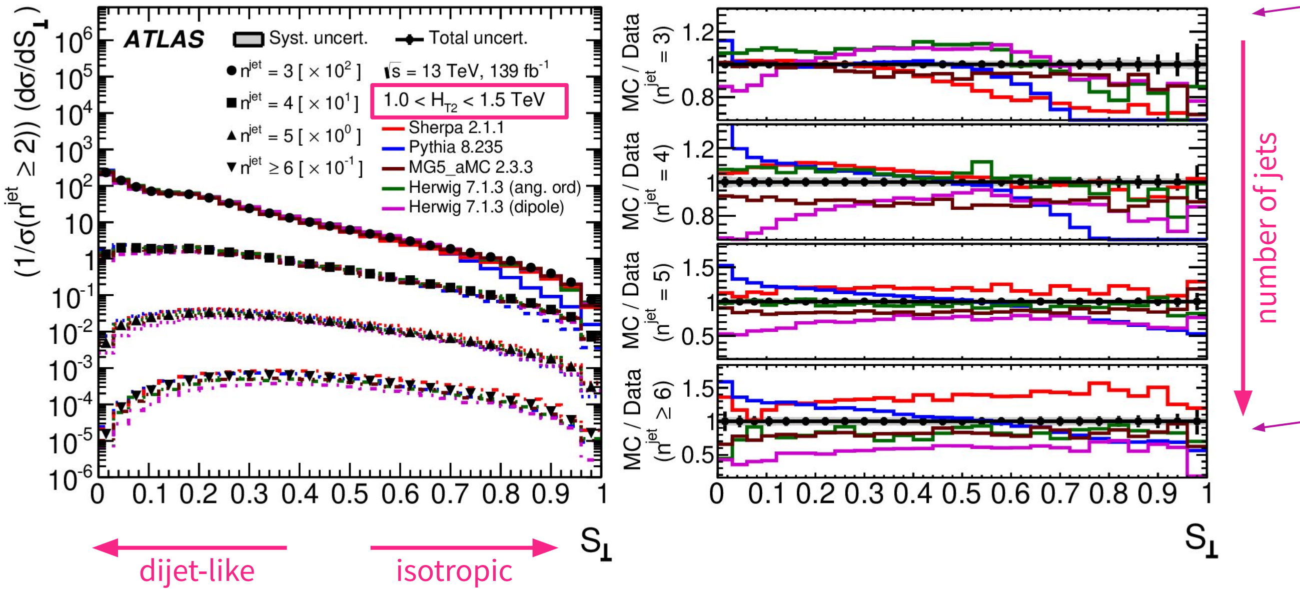

Low n^{jet} :
Pythia and Sherpa agree in the dijet-like limit, but underestimate for isotropic events.

Herwig7 and MG5_aMC are closer.

Higher n^{jet} :
Shapes are improved, but overall cross section disagreement

Hadronic event shapes

Uncertainties

- Modelling and Jet Energy Scale and Jet Energy Resolution are dominant uncertainties
- JES/JER becomes more prominent for higher n^{jet} bins
  - Dominant JES/JER uncertainty is MC mis-modelling (2007.02645)
- Total syst. uncertainty from ~1% to ~6% depending on n^{jet}

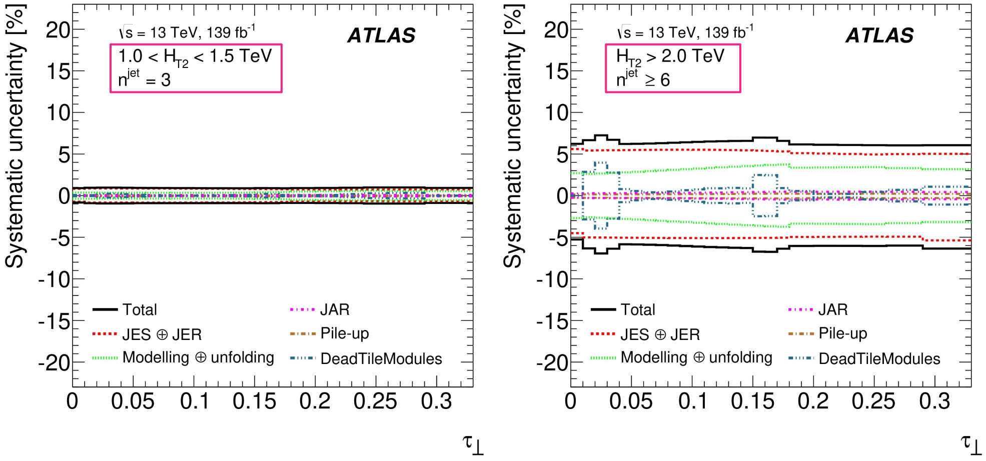

Observations

No MC predictions studied provide a good description in all regions of phase space

At low n^{jet}, Pythia and Sherpa underestimate measurements at high values of event-shape distributions.

- i.e. events in data appear to be more isotropic than predicted by simulation
- Parton shower models have trouble simulating hard and wide-angle radiation

Based on Herwig7 simulation, angle-ordered parton showers perform better than dipole-based parton showers

MG5_aMC gives best overall shape agreement

- Includes up to 4 final-state partons
- Highlights importance of ME terms beyond LO for high-p_T multijet dynamics

2004.03540

Lund jet plane

Jets can be approximated as a **core** parton **emitting** lower-energy gluons

→ The Cambridge/Aachen (C/A) reclustering algorithm combines **closest pairs** of deposits

← "Declustering" the jet in reverse populates the Lund Jet Plane (LJP) with the **widest-angle emission** at each node.

Emissions are parameterized in relative momentum fraction (z) and relative emission angle (ΔR)

A single jet can be mapped to the LJP as a set of coordinates

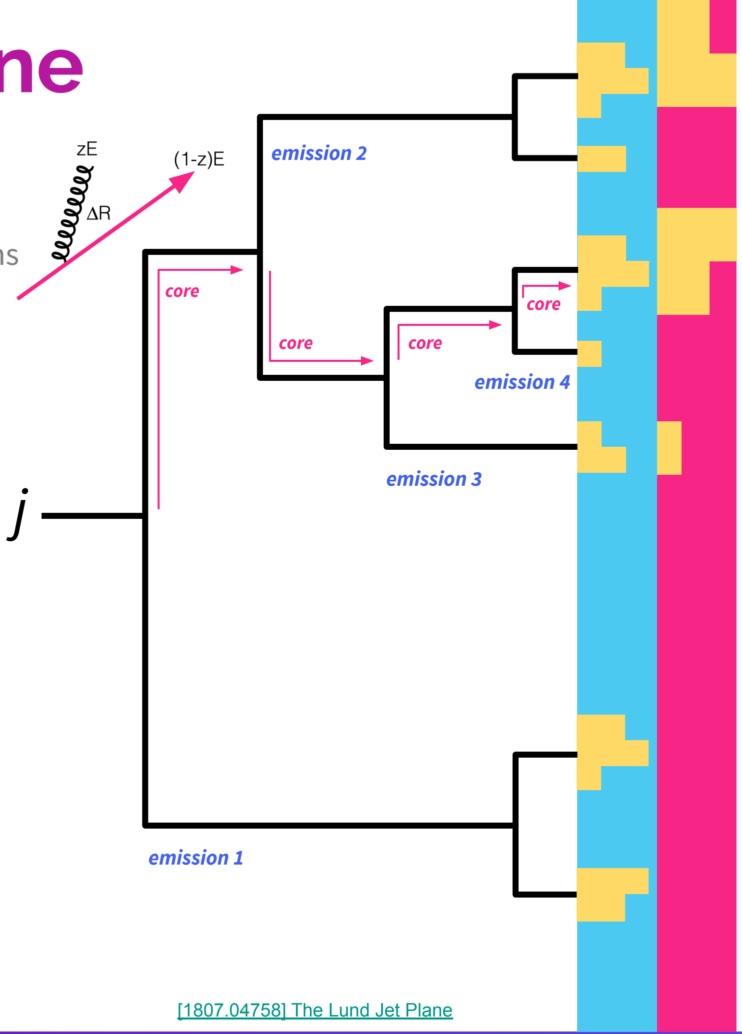

[1807.04758] The Lund Jet Plane

y-axis: ln(1/z)

z = momentum fraction of emitted gluon relative to core

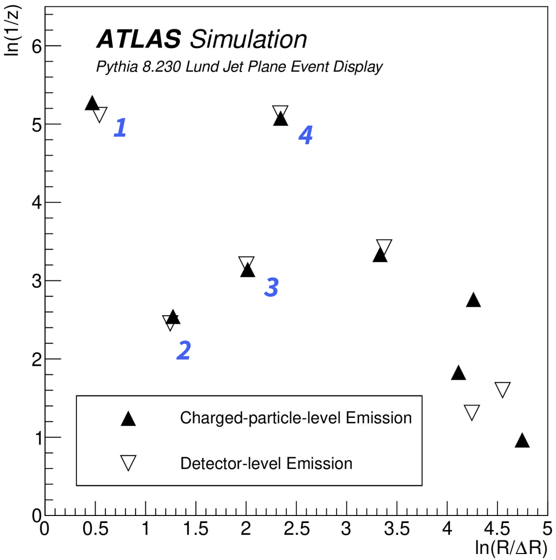

x-axis: ln(R/ΔR)

ΔR = angular separation of emitted gluon relative to core

Lund jet plane

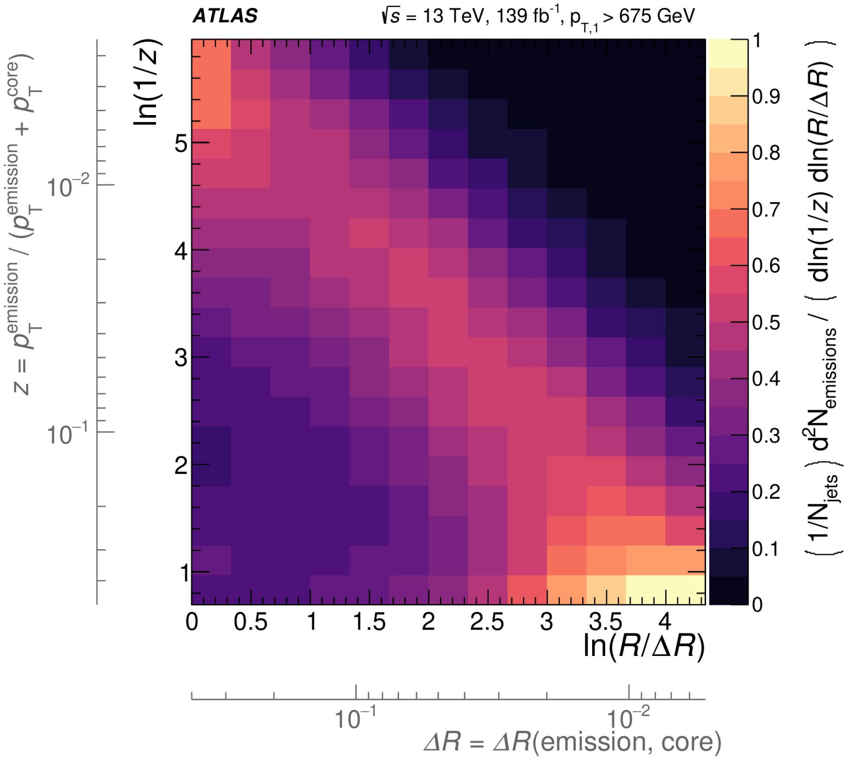

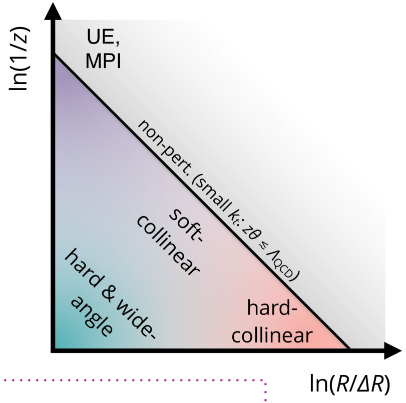

An ensemble of of jets can be plotted on the LJP and compared to simulation

~ 29.5 million (unfolded) jets collected by ATLAS are selected and plotted

Jet selection:

- Single-jet triggered
- $|\eta| < 2.1$
- $p_T^{leading} > 675$ GeV
- $p_T^{leading} / p_T^{subleading} < 1.5$

To simplify 2→2 interpretation of final state

Lund jet plane

very suppressed in NP region

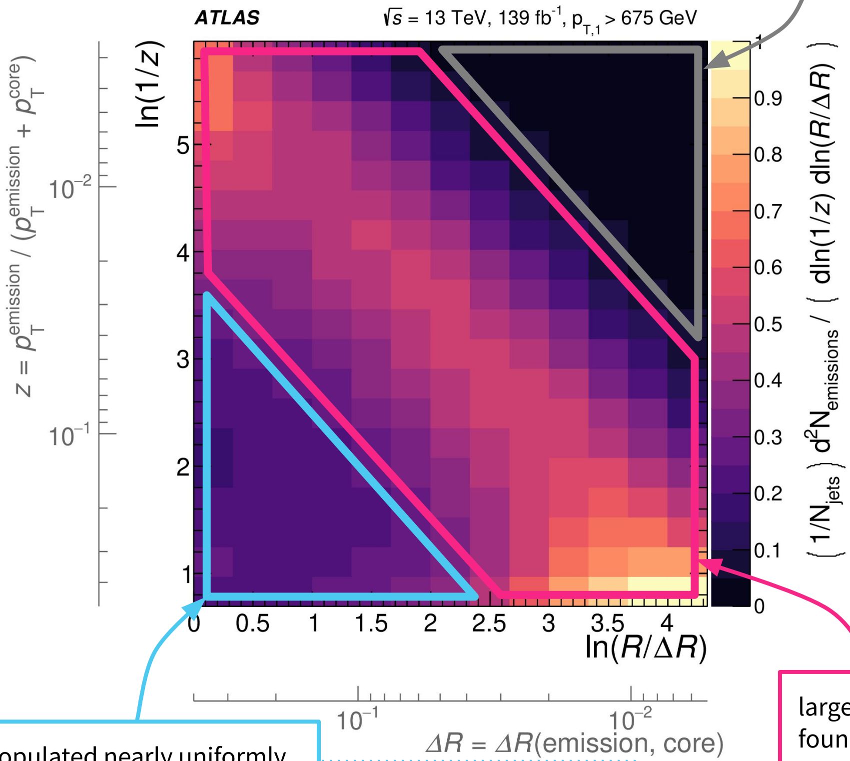

populated nearly uniformly by perturbative emissions

$$\frac{1}{N_{\text{jets}}}\frac{d^2 N_{\text{emissions}}}{d\ln(1/z)\,d\ln(R/\Delta R)} \propto \text{constant},$$

large number of emissions found at the transition to the nonperturbative regime.
α_s is enhanced for small values of k_t

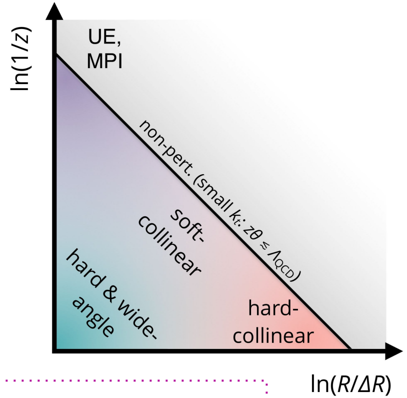

An ensemble of of jets can be plotted on the LJP and compared to simulation

~ 29.5 million (unfolded) jets collected by ATLAS are selected and plotted

Jet selection:

- Single-jet triggered
- $|\eta| < 2.1$
- $p_T^{\text{leading}} > 675$ GeV
- $p_T^{\text{leading}} / p_T^{\text{subleading}} < 1.5$

To simplify 2→2 interpretation of final state

Lund jet plane

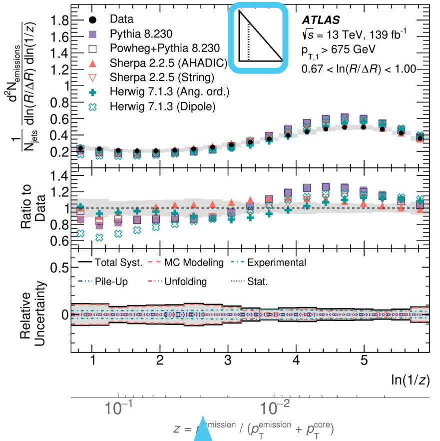

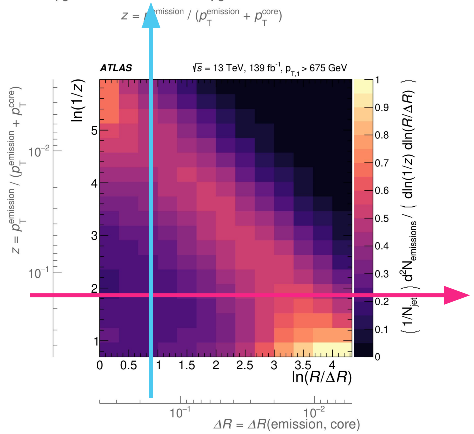

Herwig 7.1.3 (Ang. ord.)
Herwig 7.1.3 (Dipole)

Different **parton shower models** differ most significantly for **hard emissions at wide angles** (large values of k_t)

Sherpa 2.2.5 (AHADIC)
Sherpa 2.2.5 (String)

Different **hadronization models** differ most significantly for **soft collinear splittings**, at **transition to NP region** (small values of k_t)

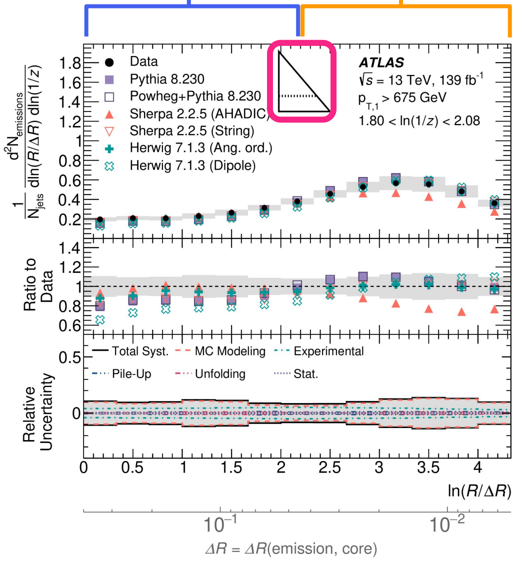

Slices of the LJP are plotted and compared to MC generators with different **parton shower** and **hadronization** models.

No single model is found to be in agreement with the measured data across the entire plane

Can be useful for tuning NP models and for constraining the parameters of advanced parton shower programs

Lund jet plane

Ratios of the LJP using different hadronization or showering algorithms **can factorize physical effects**

Parton shower ratio shows difference in harder wider-angle emissions

Hadronization ratio shows where hadronization effects are isolated

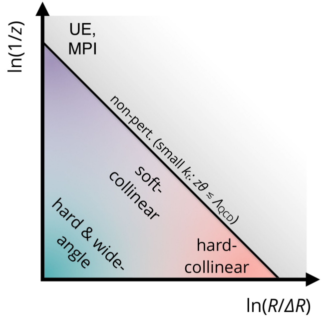

Herwig 7.1.3 +

Angle-ordered parton shower

Dipole parton shower

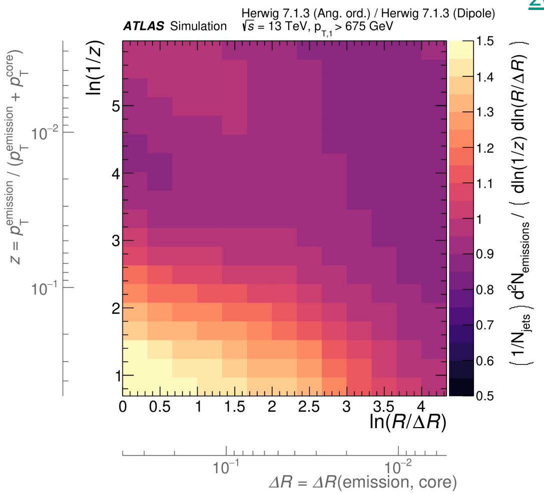

Sherpa 2.2.5 +

AHADIC cluster-based hadronization

LUND string-based hadronization

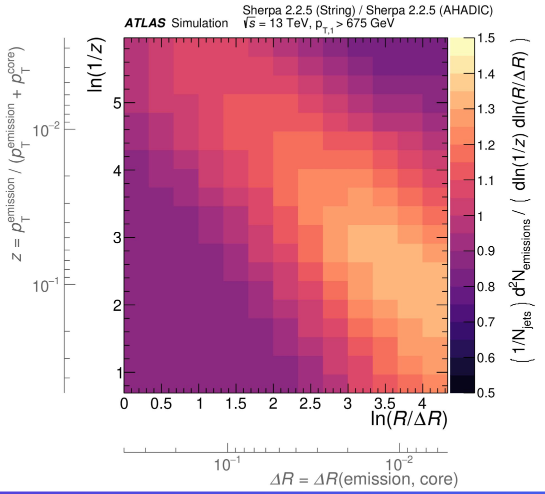

α_s measurement using (A)TEEC

Measurement of strong coupling

Uses full Run-2 dataset to measure α_s via evolution of TEEC/ATEEC with varying hard scale

Both observables are sensitive to QCD radiation and present a clear dependence with the strong coupling

Tests asymptotic freedom beyond TeV scale at NLO accuracy

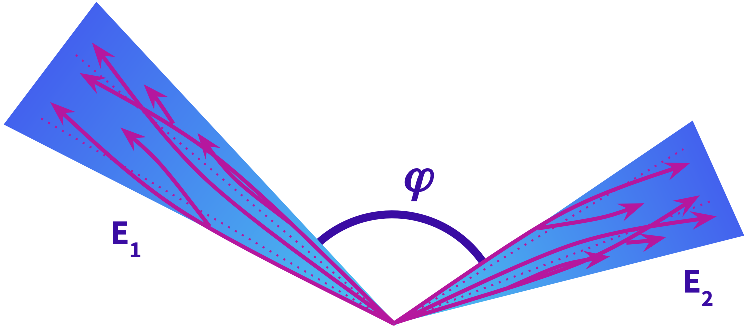

Analysis

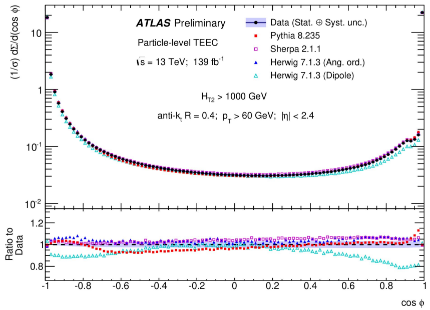

Jets:

Particle-flow, anti-k_t, R = 0.4
p_T > 60 GeV, $|\eta| < 2.4$

Events:

≥ 2 jets with H_{T2} > 1 TeV — 1006.2144
$H_{T2} = p_{T1} + p_{T2}$ is proxy for hard interaction scale Q

Unfolding:

Unfolded to particle-level using iterative Bayesian unfolding

Calculation of α_s:

(A)TEEC distributions measured inclusively and in bins of H_{T2}
$\alpha_s(m_Z)$ determined by fitting theor. predictions to distributions

TEEC — Transverse energy-energy correlation
ATEEC — Its associated azimuthal angular asymmetry

TEEC

Azimuthal distance between any two jets

$$\frac{1}{\sigma}\frac{d\Sigma}{d\cos\phi} = \frac{1}{\sigma}\sum_{i,j}\int d\sigma \frac{E_{\mathrm{T},i}E_{\mathrm{T},j}}{(E_{\mathrm{T},i}+E_{\mathrm{T},j})^2}\delta(\cos\Delta\varphi_{ij}-\cos\phi)$$

TEEC function in multi-jet events defined as the **transverse energy-weighted azimuthal angular distribution of jet pairs in the final state**

- Peaks at cos(ϕ) ≃ -1 : **back to back** two-jet events and cos(ϕ) ≃ +1 : **self correlation***
- **Central plateau** : dominated by wide-angle radiation
- MC generators match data depending on cos(ϕ) region

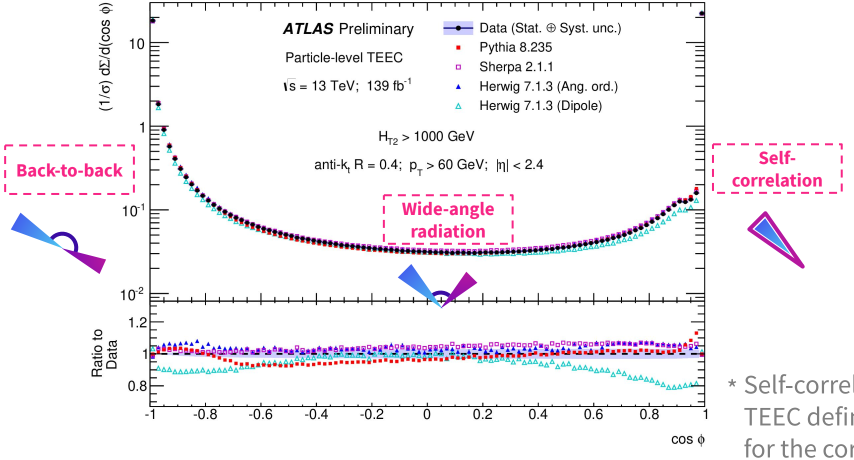

ATEEC

$$\frac{1}{\sigma}\frac{d\Sigma^{\mathrm{asymm}}}{d\cos\phi} = \frac{1}{\sigma}\left(\frac{\Sigma}{d\cos\phi}\bigg|_{\phi} - \frac{\Sigma}{d\cos\phi}\bigg|_{\pi-\phi}\right)$$

Measures the **difference between the forward (cos ϕ > 0) and the backward (cos ϕ < 0) TEEC**

- Eliminates uncertainties symmetric in cos(ϕ)
- Peaks at cos(ϕ) ≃ -1 and drops off several orders of magnitude

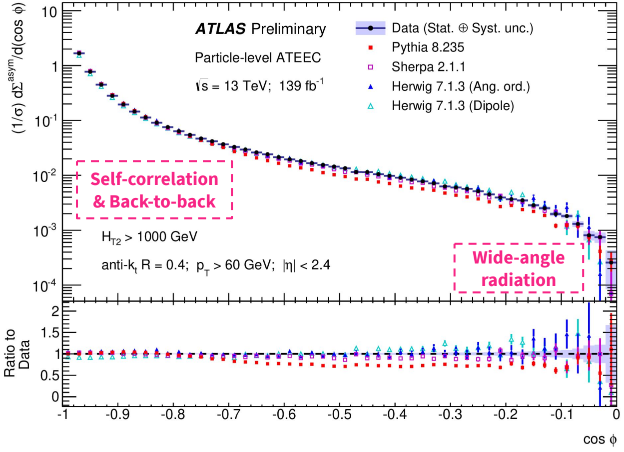

* Self-correlations are included in TEEC definition and are necessary for the correct normalization

α_s measurement using (A)TEEC

A(TEEC) binned in H_{T2} and $\alpha_s(m_Z)$ is determined by fitting theoretical predictions to the observed data

- Fit is done per-bin and globally

For each bin, $\alpha_s(m_Z)$ is evolved to $\alpha_s(Q)$ using NLO solutions to the renormalization group equation

Extends $\alpha_s(Q)$ measurement to Q > 1 TeV

- Tests RGE predictions at the highest energy scales ever!
- Agrees well with PDG world average

Comparison to previous analysis (8 TeV) arXiv:1707.02562

- Uncertainties: Stat. 1.5% → 0.5% — Syst. 5% → 2%
- Increase Q reach from .8 TeV → 4 TeV

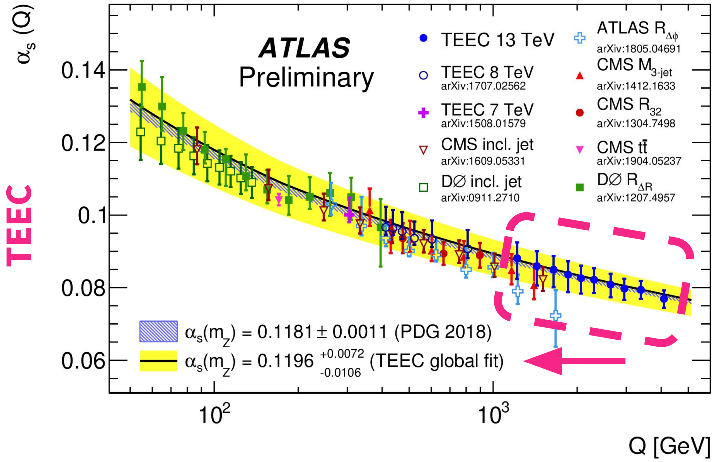

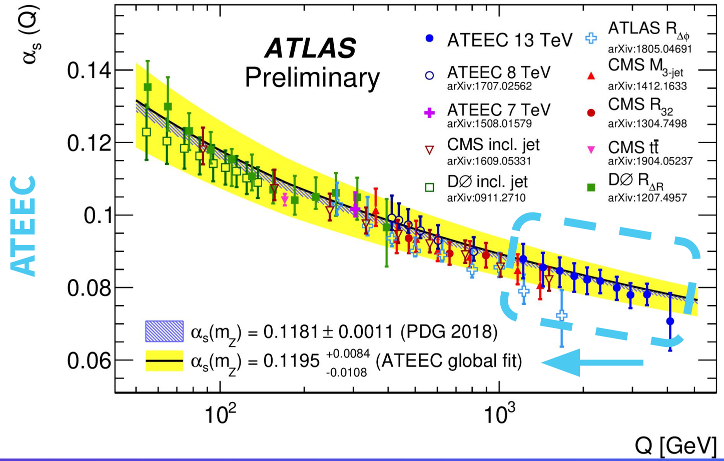

Conclusions

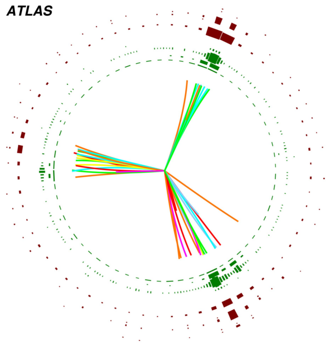

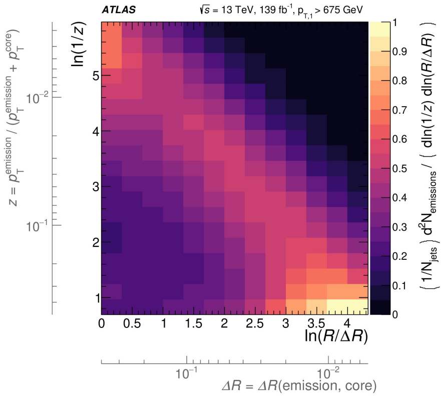

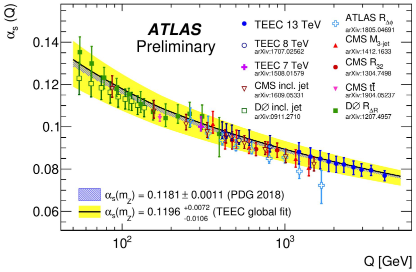

- Jet substructure and correlation measurements are used to understand and improve the performance of simulation, and to probe QCD
- Modelling uncertainties are dominant in many regions and no one generator performs well in all phase spaces
- The large quantity of events in the Run 2 dataset allows for multi-differential measurements, and precisions measurements of physical parameters

More jets & QCDin ATLAS at LHCP 2021

Nucleon Structure and Soft QCD from ATLAS

Andre Sopczak (Monday - *Nucleon Structure and Soft QCD*)

Flavour-tagging / Jet / Met performance in ATLAS and CMS

Jonathan Bossio (Thursday - *Detector performance*)

Precision QCD Measurements from ATLAS

Tibor Zenis (Thursday - *QCD: Precision Measurements*)

Results on soft QCD at LHC and Tevatron

Leszek Adamczyk (Friday - *Plenary VII: QCD Physics*)

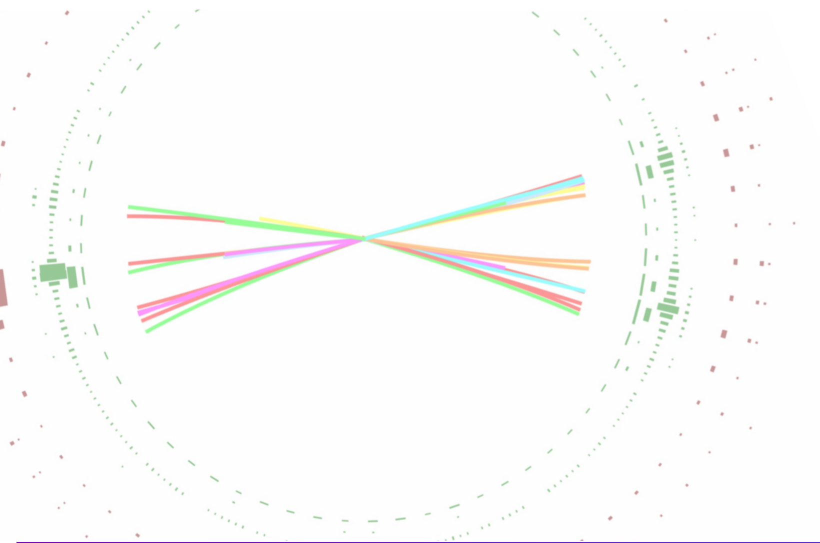

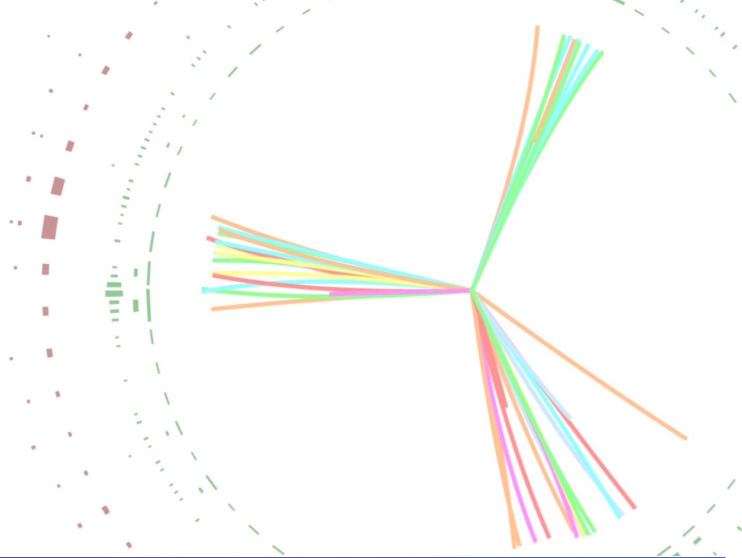

Thank you for your attention!

Additional material

[2007.12600](2007.12600)

Hadronic event shapes

Thrust

Measures back-to-back dijet-like configuration

$$T_{\perp} = \frac{\sum_i |\vec{p}_{\mathrm{T},i} \cdot \hat{n}_{\mathrm{T}}|}{\sum_i |\vec{p}_{\mathrm{T},i}|}$$

$$T_{\mathrm{m}} = \frac{\sum_i |\vec{p}_{\mathrm{T},i} \times \hat{n}_{\mathrm{T}}|}{\sum_i |\vec{p}_{\mathrm{T},i}|}$$

$\hat{n}_{\mathrm{T}}$ thrust axis – direction where jet momentum projection is maximized

$\tau_{\perp} = 1 - T_{\perp}$

Spericity tensor

$$\mathcal{M}_{xyz} = \frac{1}{\sum_i |\vec{p}_i|} \sum_i \frac{1}{|\vec{p}_i|} \begin{pmatrix} p_{\mathrm{x},i}^2 & p_{\mathrm{x},i}p_{\mathrm{y},i} & p_{\mathrm{x},i}p_{\mathrm{z},i} \\ p_{\mathrm{y},i}p_{\mathrm{x},i} & p_{\mathrm{y},i}^2 & p_{\mathrm{y},i}p_{\mathrm{z},i} \\ p_{\mathrm{z},i}p_{\mathrm{x},i} & p_{\mathrm{z},i}p_{\mathrm{y},i} & p_{\mathrm{z},i}^2 \end{pmatrix} \quad \text{eigenvalues } \{\lambda_k\}$$

Transverse spericity tensor

$$\mathcal{M}_{xy} = \frac{1}{\sum_i |\vec{p}_i|} \sum_i \frac{1}{|\vec{p}_i|} \begin{pmatrix} p_{\mathrm{x},i}^2 & p_{\mathrm{x},i}p_{\mathrm{y},i} \\ p_{\mathrm{y},i}p_{\mathrm{x},i} & p_{\mathrm{y},i}^2 \end{pmatrix} \quad \text{eigenvalues } \{\mu_k\}$$

Sphericity

$$S = \frac{3}{2}(\lambda_2 + \lambda_3)$$

Measures spherical isotropy

$$S_{\perp} = \frac{2\mu_2}{\mu_1 + \mu_2}$$

Measures planar isotropy

Aplanarity

$$A = \frac{3}{2}\lambda_3$$

Measures the containment of the radiation in a plane

C & D

Quadratic and cubic combinations of the eigenvalues

$$C = 3(\lambda_1\lambda_2 + \lambda_1\lambda_3 + \lambda_2\lambda_3)$$

3+ jet event shape

$$D = 27(\lambda_1\lambda_2\lambda_3)$$

4+ jet event shapes

Hadronic event shapes

Event shape definitions:

$\boldsymbol{S_\perp}$: Alice Collaboration, **Transverse sphericity of primary charged particles**, arXiv:1205.3963

A*, *C* and *D: CMS Collaboration, **Study of the UE in top quark pair production**, arXiv:1807.02810

$\boldsymbol{T_\perp}$, $\boldsymbol{T_m}$: CMS Collaboration, **First measurement of hadronic event shapes**, arXiv:1102.0068

$\boldsymbol{T_\perp}$: CMS Collaboration, **Event shapes and azimuthal correlations in Z + jets events**, arXiv:1301.1646

$\boldsymbol{T_\perp}$: CMS Collaboration, **Event shapes variables measured using multijet final states**, arXiv:1811.00588

$\boldsymbol{A}$, $\boldsymbol{T_m}$, $\boldsymbol{S_{\alpha,\beta}}$: C. Chen, **New approach to identifying boosted hadronically decaying particles using jet substructure**, arXiv:1112.2567

Hadronic event shapes

The dominant uncertainty is in MC mis-modelling and is taken to be the difference between the smoothed calibration curves derived from the Powheg+Pythia8 and Sherpa dijet samples. https://arxiv.org/abs/2007.02645 (Sec. 5.2.1)

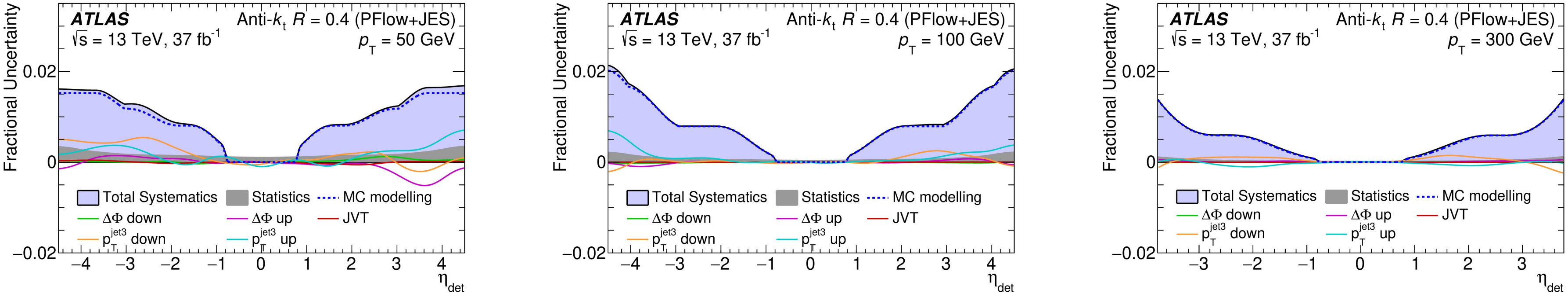

Lund jet plane

Why this choice of axes?

The LJP is sometimes depicted with the y-axis representing $\ln(k_t)$.

The choice of using z instead of k_t is to decouple the angular (x-axis) and momentum (y-axis) measurements as the resolution of each can differ substantially.

Historically, both choices of axes have been used.

$k_t \sim z^*\Delta R$

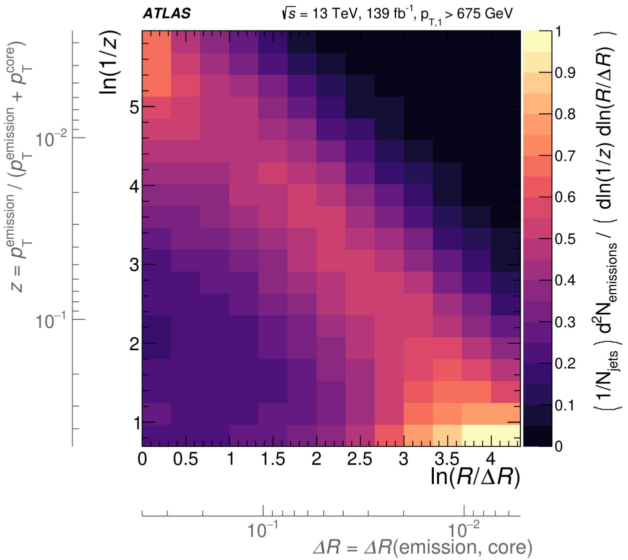

Discussion of variables: arXiv:1807.04758 Sec. 2.1

α_s measurement using (A)TEEC

Dominant systematics

TEEC systematic uncertainties are dominated by
Jet Energy Scale (< 2%) and
modelling of the strong interaction (< 2%)

ATEEC systematic uncertainties are dominated by
Jet Energy Scale (< 1%) and
Jet Energy Resolution (< 1%)

Other sources of systematic uncertainty include:
Jet Angular Resolution (<0.5%) and
Unfolding uncertainty (negligible)

TEEC

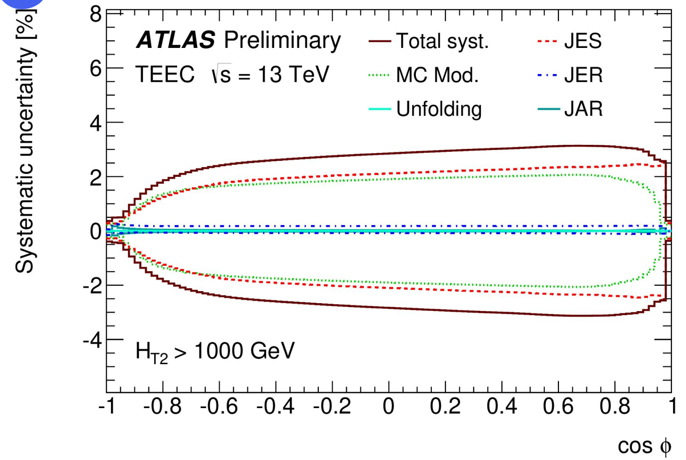

ATEEC

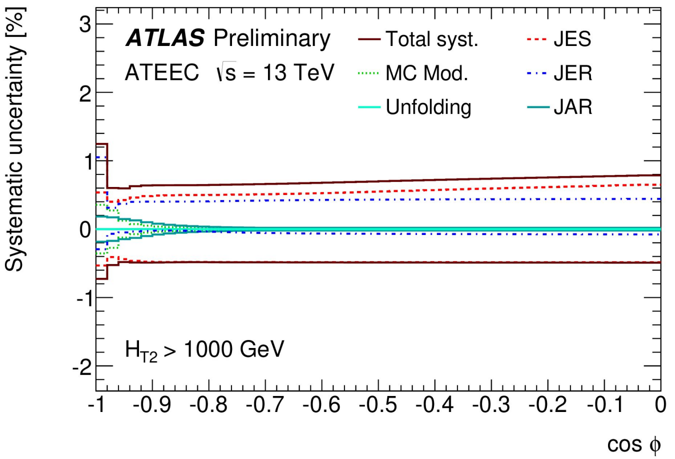

α_s measurement using (A)TEEC

The values of $\alpha_s(m_Z)$ determined from fits to the (A)TEEC functions, in inclusive and exclusive H_{T2} bins, and global fit.

Scale:
The renormalisation scale is set for each event to the scalar sum of the transverse momenta of all final-state partons, $\mu_R = \hat{H}_T$, while the factorisation scale is set to half this scale, $\mu_F = \hat{H}_T/2$.
[arXiv:1807.03692, arXiv:2007.02645]

TEEC

$\langle Q \rangle$ [GeV]	$\alpha_s(m_Z)$ value (MMHT 2014)	χ^2/N_{dof}
Global	0.1196 ± 0.0001 (stat.) ± 0.0004 (syst.) $^{+0.0071}_{-0.0104}$ (scale) ± 0.0011 (PDF) ± 0.0002 (NP)	235.8 / 347
Inclusive	0.1208 ± 0.0002 (stat.) ± 0.0006 (syst.) $^{+0.0081}_{-0.0101}$ (scale) ± 0.0009 (PDF) ± 0.0002 (NP)	42.7 / 91
1219	0.1206 ± 0.0002 (stat.) ± 0.0006 (syst.) $^{+0.0083}_{-0.0105}$ (scale) ± 0.0009 (PDF) ± 0.0003 (NP)	18.6 / 51
1434	0.1191 ± 0.0003 (stat.) ± 0.0007 (syst.) $^{+0.0080}_{-0.0101}$ (scale) ± 0.0010 (PDF) ± 0.0002 (NP)	18.0 / 51
1647	0.1195 ± 0.0002 (stat.) ± 0.0007 (syst.) $^{+0.0077}_{-0.0094}$ (scale) ± 0.0011 (PDF) ± 0.0002 (NP)	38.2 / 51
1856	0.1186 ± 0.0003 (stat.) ± 0.0008 (syst.) $^{+0.0076}_{-0.0094}$ (scale) ± 0.0011 (PDF) ± 0.0004 (NP)	25.9 / 51
2064	0.1183 ± 0.0004 (stat.) ± 0.0010 (syst.) $^{+0.0071}_{-0.0084}$ (scale) ± 0.0012 (PDF) ± 0.0005 (NP)	22.4 / 27
2300	0.1192 ± 0.0004 (stat.) ± 0.0011 (syst.) $^{+0.0066}_{-0.0075}$ (scale) ± 0.0012 (PDF) ± 0.0004 (NP)	21.3 / 27
2636	0.1185 ± 0.0004 (stat.) ± 0.0012 (syst.) $^{+0.0064}_{-0.0072}$ (scale) ± 0.0012 (PDF) ± 0.0001 (NP)	22.0 / 27
2952	0.1179 ± 0.0005 (stat.) ± 0.0014 (syst.) $^{+0.0059}_{-0.0064}$ (scale) ± 0.0013 (PDF) ± 0.0003 (NP)	25.0 / 27
3383	0.1194 ± 0.0007 (stat.) ± 0.0014 (syst.) $^{+0.0052}_{-0.0052}$ (scale) ± 0.0013 (PDF) ± 0.0002 (NP)	15.3 / 13
4095	0.1167 ± 0.0010 (stat.) ± 0.0014 (syst.) $^{+0.0050}_{-0.0053}$ (scale) ± 0.0015 (PDF) ± 0.0003 (NP)	13.5 / 13

Table 2: Values of the strong coupling constant at the Z boson mass scale, $\alpha_s(m_Z)$, obtained from fits to the TEEC function using MMHT 2014 parton distribution functions. The values of the average interaction scale $\langle Q \rangle$ are shown in the first column, while the values of the χ^2 function at the minimum are shown in the third column. The uncertainty referred to as NP is the one related to the non-pQCD corrections.

ATEEC

$\langle Q \rangle$ [GeV]	$\alpha_s(m_Z)$ value (MMHT 2014)	χ^2/N_{dof}
Global	0.1195 ± 0.0002 (stat.) ± 0.0006 (syst.) $^{+0.0084}_{-0.0106}$ (scale) ± 0.0009 (PDF) ± 0.0003 (NP)	254.1 / 173
Inclusive	0.1198 ± 0.0002 (stat.) ± 0.0006 (syst.) $^{+0.0078}_{-0.0095}$ (scale) ± 0.0010 (PDF) ± 0.0002 (NP)	46.3 / 45
1219	0.1202 ± 0.0003 (stat.) ± 0.0006 (syst.) $^{+0.0079}_{-0.0098}$ (scale) ± 0.0010 (PDF) ± 0.0002 (NP)	25.7 / 25
1434	0.1184 ± 0.0003 (stat.) ± 0.0007 (syst.) $^{+0.0078}_{-0.0098}$ (scale) ± 0.0011 (PDF) ± 0.0002 (NP)	35.6 / 25
1647	0.1188 ± 0.0004 (stat.) ± 0.0007 (syst.) $^{+0.0073}_{-0.0087}$ (scale) ± 0.0012 (PDF) ± 0.0001 (NP)	41.9 / 25
1856	0.1177 ± 0.0006 (stat.) ± 0.0008 (syst.) $^{+0.0072}_{-0.0083}$ (scale) ± 0.0013 (PDF) ± 0.0006 (NP)	24.6 / 25
2064	0.1174 ± 0.0008 (stat.) ± 0.0009 (syst.) $^{+0.0069}_{-0.0078}$ (scale) ± 0.0013 (PDF) ± 0.0007 (NP)	18.7 / 13
2300	0.1185 ± 0.0009 (stat.) ± 0.0010 (syst.) $^{+0.0063}_{-0.0067}$ (scale) ± 0.0014 (PDF) ± 0.0005 (NP)	22.5 / 13
2636	0.1166 ± 0.0016 (stat.) ± 0.0012 (syst.) $^{+0.0062}_{-0.0066}$ (scale) ± 0.0015 (PDF) ± 0.0000 (NP)	21.7 / 13
2952	0.1141 ± 0.0029 (stat.) ± 0.0013 (syst.) $^{+0.0062}_{-0.0069}$ (scale) ± 0.0018 (PDF) ± 0.0003 (NP)	15.2 / 13
3383	0.1164 ± 0.0043 (stat.) ± 0.0015 (syst.) $^{+0.0050}_{-0.0044}$ (scale) ± 0.0017 (PDF) ± 0.0001 (NP)	6.3 / 6
4095	0.1029 ± 0.0163 (stat.) ± 0.0014 (syst.) $^{+0.0066}_{-0.0012}$ (scale) ± 0.0010 (PDF) ± 0.0003 (NP)	5.9 / 6

Table 3: Values of the strong coupling constant at the Z boson mass scale, $\alpha_s(m_Z)$, obtained from fits to the ATEEC function using MMHT 2014 parton distribution functions. The values of the average interaction scale $\langle Q \rangle$ are shown in the first column, while the values of the χ^2 function at the minimum are shown in the third column. The uncertainty referred to as NP is the one related to the non-pQCD corrections.